Predictive model of persistence in H2RG detectors

S. Tulloch,& E. George 2019, arXiv:1908.06469

Infrared hybridized detectors are widely used in astronomy, and their performance can be degraded by image persistence. This results in remnant images that can persist in the detector for many hours, contaminating any subsequent low-background observations. A different but related problem is reciprocity failure whereby the detector is less sensitive to low flux observations. It is demonstrated that both of these problems can be explained by trapping and detrapping currents that move charge back and forward across the depletion region boundary of the photodiodes within each pixel. These traps have been characterized in one 2.5 μm and two 5.3 μm cutoff wavelength Teledyne H2RG detectors. We have developed a behaviour model of these traps using a 5-pole Infinite Impulse Response digital filter. This model allows the trapped charge in a detector to be constantly calculated for arbitrary exposure histories, providing a near real-time correction for image persistence.

- パーシステンス

⇨ 電荷の蓄積に伴う空乏層の縮小の際に格子欠陥に囚われた電荷が時間を経た後に解放されることが原因

この論文ではCRIRES+5.3um, ERIS5.3um,2.5umの3つのH2RGのパーシステンス特性の評価とモデル化をおこなっている。

- データ取得

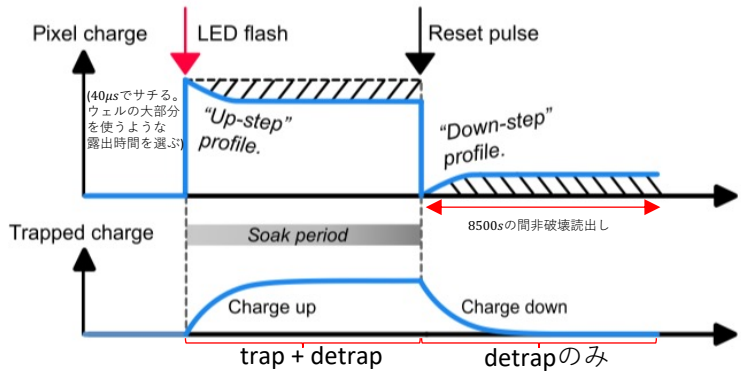

Fig. 5 The LED method used to probe the trapping and detrapping time constants. Key parts of the trapped charge and signal level profiles are shown labeled.

- trap,detrap時定数の測定

Charge down phaseの画像の信号を以下の関数でフィッティング

$$Q(t) = \sum_{i=1}^{5} \left\{ N_i \left[1 - \exp\left(-\frac{t}{\tau_i} \right) \right] \right\} \quad (\tau_i = 10^{i-1})$$

この時のN_iがそれぞれの時定数ビンを持つ電荷数となる。

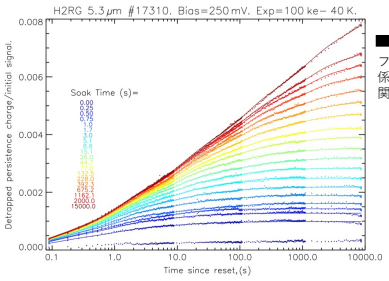

Fig. 8 Family of detrapping profiles for the CRIRES+ detector at a constant exposure level of 100 ke⁻ applied for a soak time that varied between 0 and 15,000 s. The line fits to the data use Eq. (1).

フィッティングの係数をsoak timeの関数としてプロット

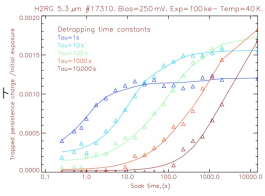

Fig. 9 The effect of increasing soak time on the amount of charge trapped in each detrapping time constant bin. These data are obtained by applying the exponential analysis technique to the data in Fig. 8.

Fig. 10より、$\tau_{charge\ up} = \tau_{detrap}$

⇨ charge up(trap+detrap)の時定数がdetrapの時定数と同じなので$\tau_{trap} \gg \tau_{detrap}$

さらにフィッティングをし、detrapping time const.とトラップされる電荷が平衡状態になる時定数(charge-up time)の関係をプロット

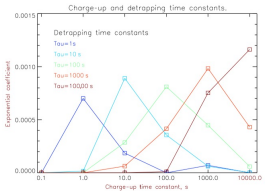

Fig. 10 Relationship between detrapping and charge-up time constants. This graph finally establishes the link between trap time constants in the postreset detrapping phase and those in the charge-up soak phase. These data are obtained by applying the exponential analysis technique to the plots in Fig. 9. Both plots use the same vertical axis units.

- トラップモデル

仮定:

1. detrap電流は充填されたトラップ数に比例
2. トラップ電流はピクセル内の光電子数に比例
3. 充填トラップ数はtrap電流とdetrap電流の差の時間積分

モデル:

各時定数について右図のようなRC回路をでモデル化できる。その時、

1. 充填トラップ数：コンデンサ上の電荷
2. Trap電流: 電流源の電流の大きさ
3. Detrap電流：抵抗を通る電流の大きさ

で表すことができる。複数の時定数がある場合は、時定数の線形和で書くことができる。

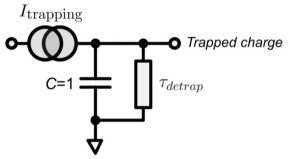

Fig. 11 Symbolic model of an ensemble of persistence-inducing traps.

- 光電子数 vs detrap電子数

※Soak timeは1000sに固定

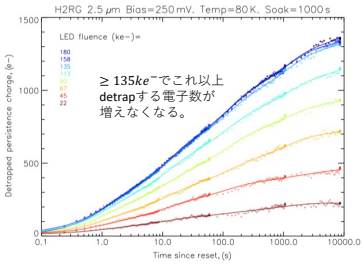

Fig. 12 Detrapping profiles with constant soak and variable LED fluence for the ERIS 2.5-μm detector. The line fits to the data use Eq. (1).

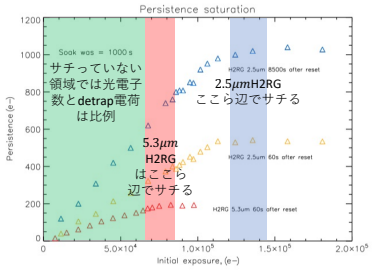

Fig. 13 Persistence saturation at full well in the ERIS 2.5-and 5.3-μm detectors. Exposure levels were calculated from a combination of LED on-time and its brightness in e^-/ms at low flux levels. Data at 8500 s for the 5.3-μm device were not included due to the difficulty of accurately removing the high instrumental background contribution.

- フォトントランスファー

トラップに出入りする電子はそれぞれ異なるコンバージョンゲインを持つ

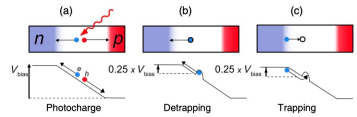

Fig. 2 (a)–(c) Charge movement to and from the DR. Trapping and detrapping charge carriers have fractional effective charge. This example shows the behavior of a trap that is 1/4 of the way across the DR. In reality, the trap positions are widely distributed. $\Delta E = CV\Delta V$

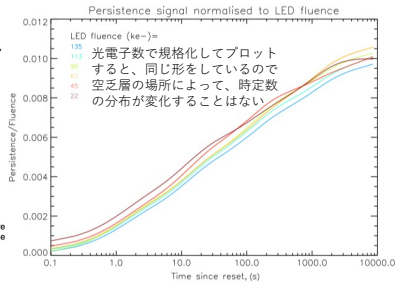

Fig. 14 Detrapping time constant invariability with exposure level. The detrapping profiles shown in Fig. 12 were divided by the initial exposure level to reveal any possible time-constant changes with exposure level.

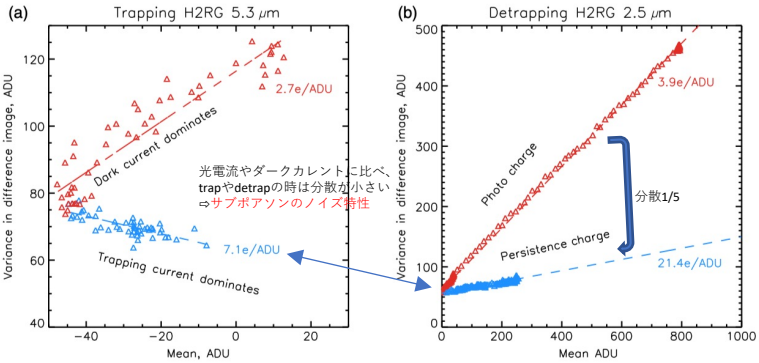

Fig. 16 Photon transfer of persistence. (a) (ERIS 5.3-μm device) the statistics of the trapping current in blue and the dark current in red. The negative gradient of the trapping current statistics is due to the mean signal on the pixel actually decreasing due to the trapping. Dark current of course acts to increase the signal. (b) (ERIS 2.5-μm device) the statistics of detrapping current in blue and photocharge/dark current in red. All of these act to increase the signal on the pixel.

- Reciprocity failure

$\tau_{charge\ up} = \tau_{detrap}$なので、up-step profileはdown-step profileを反映したものになるはず

⇨ 実際は対称ではなく、up-step profileは、特にflashから長時間が経過した後はリーク電流によって支配される

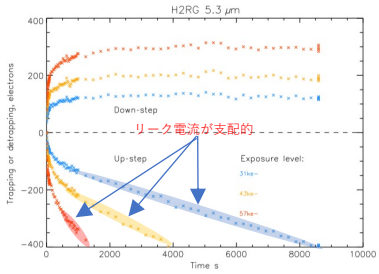

Fig. 17 Charge loss from a pixel due to trapping currents during the "up-step" exposure phase and charge gain due to detrapping currents during the "down-step." The up-step runs reveal an additional leakage current in the pixel. Refer to Fig. 5 for an explanation of the terms. Data obtained using the ERIS detector.

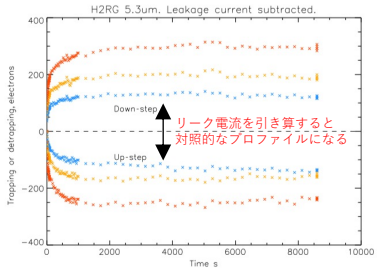

Fig. 18 Symmetry of "up-step" exposure phase and charge gain due to detrapping currents during the "down-step," as shown in Fig. 17, once the leakage current has been subtracted. Refer to Fig. 17 for the color codes of the three plot groups.